

Delayed Feedback Controller for Stabilizing Subsynchronous Oscillations in Power Systems

Yaşar Küçükefe¹ and Adnan Kaypmaz²

¹National Power Enerji, Tekirdağ, Turkey
yasar.kucukefe@ieee.org

²Istanbul Technical University, İstanbul, Turkey
kaypmaz@elk.itu.edu.tr

Abstract

This paper presents a novel controller based on the delayed feedback control theory for stabilizing unstable torsional oscillations caused by Subsynchronous Resonance (SSR) in power systems. The first system of the IEEE Second Benchmark Model, which consists of a synchronous generator connected to an infinite busbar through two parallel transmission lines, one of which is equipped with a series capacitor, is used to evaluate the controller's effectiveness. Dynamics of the generator damper windings and the Automatic Voltage Regulator (AVR) are included in the nonlinear model. The controller uses the synchronous generator rotor angular speed as the only input. The difference between the input signal's value τ -time in the past and its current value is multiplied with a gain to obtain the controller output, which is then combined into the AVR as the stabilizing signal. The effectiveness of the proposed controller in damping the torsional oscillations is demonstrated via time-domain simulations in MATLAB-Simulink. The controller performance index is also introduced to evaluate the effectiveness of the controller.

1. Introduction

Series capacitor compensation of AC transmission lines is an effective way of increasing load carrying capacity and enhancing transient stability. It is known that subsynchronous resonance (SSR) can occur in electric power systems consisting of turbine-generators connected to transmission lines with series capacitors. Unless adequate measures are implemented, SSR can lead to turbine-generator shaft failures as occurred at the Mohave Power Plant in Southern Nevada in the USA in 1970 [1]. IEEE SSR Working Group has constructed three benchmark models for computer simulation of the SSR [2, 3]. Analytical tools for studying the SSR involve frequency scanning, eigenvalue technique, time domain simulation programs [4] and the complex torque coefficient method [5, 6].

A single-machine-infinite-busbar (SMIB) power system with series capacitor compensation is inherently nonlinear and can be modeled by sets of ordinary differential equations. The nonlinear model including the dynamics of the turbine-generator shaft system can be analyzed by using the methods of the nonlinear theory. Zhu et al. [7] demonstrated the existence of Hopf bifurcation in a SMIB power system susceptible to SSR. Iravani et al. [8] investigated the Hopf bifurcation phenomenon of the torsional dynamics. Harb [9] employed the bifurcation theory to investigate the complex dynamics of the SSR.

Countermeasures against SSR include implementations and proposals such as the blocking filters [10], excitation controllers [11], static VAR compensators [12], SSR damping controller integrated in a static synchronous compensator (STATCOM) [13], NGH damping scheme [14] and Bifurcation control [15].

Delayed feedback control [16] is a simple and efficient method to stabilize both unstable periodic orbits (UPO) embedded in the strange attractors of chaotic systems [17] and unstable steady states [18]. Also known as Time Delay Auto-Synchronization (TDAS), this control scheme makes use of the current state of a system and its state τ -time unit in the past to generate a control signal. In the case with UPOs, the most efficient performance of TDAS controller can be obtained if time delay (τ) corresponds to an integer multiple of the minimal period of the unstable orbit. The method works best if τ is set a value related to intrinsic characteristic time scale given by the imaginary part of the system's eigenvalue in the case of unstable steady states [19].

In this paper, we present a novel controller based on the delayed feedback control theory. The proposed controller uses the synchronous generator rotor angular speed signal as the only input, which is an accessible state variable. The output of the controller is combined into the AVR as the stabilizing signal. The first system of the IEEE second benchmark model for SSR studies is used to evaluate the controller's performance. The controller parameters have been determined by evaluating the dynamic response for a range of parameters. Time domain simulations using the nonlinear model are presented to demonstrate that the proposed controller can effectively stabilize the unstable torsional oscillations.

This paper is organized as follows. The SMIB power system under study is described in Section II. Delayed Feedback Controller (DFC) is presented in Section III. Then in Section IV, its effectiveness in stabilizing unstable torsional oscillations cause by the SSR is demonstrated via time domain simulations in MATLAB-Simulink.

2. System Description and Modeling

The complete nonlinear model representing the dynamics of the electrical and mechanical systems of the first system of the IEEE second benchmark model for SSR studies has been developed in MATLAB, using direct and quadrature d-q axes and Park's transformation [20].

In the nonlinear model, we have included the dynamics of the automatic voltage regulator and the generator rotor damper windings on the d-q axes. On the other hand, the saturation effects and the governor dynamics have been neglected. The model parameters are given in the Appendix.

2.1. Electrical System

Fig.1 shows the first system of the IEEE second benchmark model for SSR studies. It is a SMIB power system, which consists of a synchronous generator connected to an infinite busbar through two parallel transmission lines. Adjustable series capacitor compensation is applied in one of the parallel transmission lines.

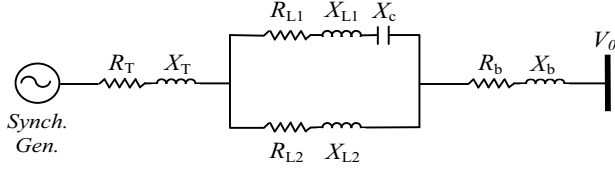


Fig. 1. First system of the IEEE second benchmark model

Defining the state variables as $\mathbf{i}_g = [i_d \ i_q \ i_f \ i_{kq} \ i_{kd}]^T$, $\mathbf{i}_g \in \mathbb{R}^5$, and $\mathbf{V}_c = [V_{cd} \ V_{cq}]^T$, $\mathbf{V}_c \in \mathbb{R}^2$, the equations in state space form can be written as:

$$\frac{d\mathbf{i}_g}{dt} = \mathbf{B}^{-1} \omega_b (\mathbf{C} \mathbf{i}_g + \mathbf{D}) \quad (1)$$

$$\frac{d\mathbf{V}_c}{dt} = \omega_b (\mathbf{E} \mathbf{i}_g + \mathbf{F} \mathbf{V}_c) \quad (2)$$

where

$$\mathbf{B} = \begin{bmatrix} -(X_d + X_E) & 0 & X_{afd} & 0 & X_{akd} \\ 0 & -(X_q + X_E) & 0 & X_{akq} & 0 \\ -X_{afd} & 0 & X_{ffd} & 0 & X_{fkd} \\ 0 & -X_{akq} & 0 & X_{kkq} & 0 \\ -X_{akd} & 0 & X_{fkd} & 0 & X_{kkd} \end{bmatrix} \quad (3)$$

$$\mathbf{C} = \begin{bmatrix} (r_a + R_E) & -(X_E + \omega_r X_q) & 0 & \omega_r X_{akq} & 0 \\ (X_E + \omega_r X_d) & (r_a + R_E) & -\omega_r X_{afd} & 0 & -\omega_r X_{akd} \\ 0 & 0 & -r_{fd} & 0 & 0 \\ 0 & 0 & 0 & -r_{kq} & 0 \\ 0 & 0 & 0 & 0 & -r_{kd} \end{bmatrix} \quad (4)$$

$$\mathbf{D} = \begin{bmatrix} V_0 \sin(\delta_r) + V_{cd} \\ V_0 \cos(\delta_r) + V_{cq} \\ r_{fd} E_{fd} / X_{afd} \\ 0 \\ 0 \end{bmatrix} \quad (5)$$

$$X_E = X_T + kX_{L1} + X_b \quad (6)$$

$$R_E = R_T + kR_{L1} + R_b \quad (7)$$

$$\mu = X_c / X_{L1} \quad (8)$$

$$k = \frac{\sqrt{R_2^2 + X_{L2}^2}}{\sqrt{(R_1 + R_2)^2 + (X_{L1} + X_{L2} - \mu X_{L1})^2}} \quad (9)$$

$$\mathbf{E} = \begin{bmatrix} \mu k X_{L1} & 0 & 0 & 0 & 0 \\ 0 & \mu k X_{L1} & 0 & 0 & 0 \end{bmatrix} \quad (10)$$

$$\mathbf{F} = \begin{bmatrix} 0 & 1 \\ -1 & 0 \end{bmatrix} \quad (11)$$

2.2. Mechanical System

The single shaft turbine generator mechanical system consists of a high-pressure (HP) turbine, a low-pressure turbine (LP), a generator and an exciter as shown in Fig.2. K, D and M parameters represent the spring coefficient, the damping coefficient and the inertia constant of the corresponding shaft section, respectively.

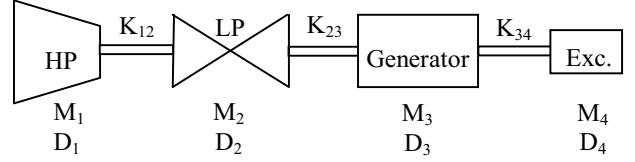


Fig. 2. Schematic diagram of the mechanical system consisting of a high-pressure (HP) turbine, a low-pressure turbine (LP), a generator and an exciter

Defining $\mathbf{R}_s = [\omega_1 \ \theta_1 \ \omega_2 \ \theta_2 \ \omega_r \ \delta_r \ \omega_4 \ \theta_4]^T$, $\mathbf{R}_s \in \mathbb{R}^8$, the equations in state space representation form can be written as follows:

$$\frac{d\mathbf{R}_s}{dt} = \mathbf{G} \mathbf{R}_s + \mathbf{H} \quad (12)$$

where

$$\mathbf{G} = \begin{bmatrix} -D_1 & -K_{12} & 0 & K_{12} & 0 & 0 & 0 & 0 \\ M_1 & M_1 & 0 & M_1 & 0 & 0 & 0 & 0 \\ \omega_b & 0 & 0 & 0 & 0 & 0 & 0 & 0 \\ 0 & K_{12} & -D_2 & -(K_{12} + K_{23}) & 0 & K_{23} & 0 & 0 \\ 0 & M_2 & M_2 & M_2 & 0 & M_2 & 0 & 0 \\ 0 & 0 & \omega_b & 0 & 0 & 0 & 0 & 0 \\ 0 & 0 & 0 & K_{23} & -D_3 & -(K_{23} + K_{34}) & 0 & K_{34} \\ 0 & 0 & 0 & M_3 & M_3 & M_3 & 0 & M_3 \\ 0 & 0 & 0 & 0 & \omega_b & 0 & 0 & 0 \\ 0 & 0 & 0 & 0 & 0 & K_{34} & -D_4 & -K_{34} \\ 0 & 0 & 0 & 0 & 0 & M_4 & M_4 & M_4 \\ 0 & 0 & 0 & 0 & 0 & 0 & \omega_b & 0 \end{bmatrix} \quad (13)$$

$$\mathbf{H} = \begin{bmatrix} D_1 \\ M_1 \\ -\omega_b \\ D_2 \\ M_2 \\ -\omega_b \\ \frac{(T_m - T_e + D_3)}{M_3} \\ -\omega_b \\ D_4 \\ M_4 \\ -\omega_b \end{bmatrix}^T \quad (14)$$

In (14), T_e represents the electromechanical torque and it is expressed as follows:

$$T_e = (X_q - X_d) i_d i_q + X_{afd} i_f i_q - X_{akq} i_{kq} i_d + X_{akd} i_{kd} i_q \quad (15)$$

2.3. Excitation System with AVR

The excitation system with AVR of type DC1A described in [21] is incorporated into the model. Fig.3 shows the block diagram of the excitation system with AVR. The effect of AVR limiters is included in the model.

Defining $\mathbf{V}_{exc} = [V_c \ V_f \ V_R \ E_{fd}]^T$, $\mathbf{V}_{exc} \in \mathbb{R}^4$, the state equations describing the dynamics of the excitation system with AVR can be written as follows:

$$\frac{d\mathbf{V}_{exc}}{dt} = \mathbf{P} \mathbf{V}_{exc} + \mathbf{Q} \quad (16)$$

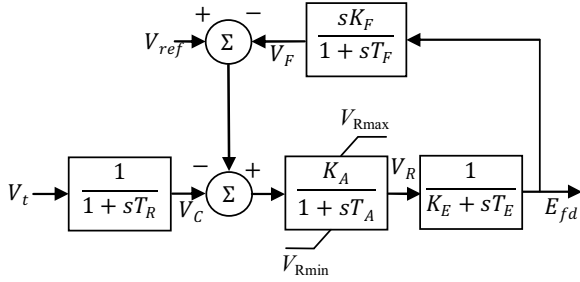


Fig. 3. Block diagram of the excitation system with AVR

Where

$$P = \begin{bmatrix} -\frac{1}{T_R} & 0 & 0 & 0 \\ 0 & -\frac{1}{T_F} & \frac{K_F}{T_F T_E} & -\frac{K_F K_E}{T_F T_E} \\ -\frac{K_A}{T_A} & -\frac{K_A}{T_A} & -\frac{1}{T_A} & 0 \\ 0 & 0 & \frac{1}{T_E} & -\frac{K_E}{T_E} \end{bmatrix} \quad (17)$$

$$Q = \left[\frac{V_t}{T_R} \quad 0 \quad \left(\frac{K_A}{T_A} V_{ref} \right) \quad 0 \right]^T \quad (18)$$

V_t in (18) is the generator terminal voltage. Neglecting the transients, V_t can be expressed as:

$$V_t = \sqrt{((-r_a i_d + X_q i_q)^2 + (-r_a i_q - X_d i_d + X_{afd} i_{fd})^2)} \quad (19)$$

2.4. Complete Mathematical Model

We define the state vector $\mathbf{x} = [i_g^T \ V_c^T \ R_s^T \ V_{exc}^T]^T$, $\mathbf{x} \in \mathbb{R}^{19}$ and combine (1-2), (12) and (16) as:

$$\dot{\mathbf{x}} = \begin{bmatrix} B^{-1} \omega_b (C i_g + D) \\ \omega_b (E i_g + F V_c) \\ G R_s + H \\ P V_{exc} + Q \end{bmatrix} \quad (20)$$

3. Modal Analysis

Oscillatory modes of the model depending on the series compensation factor ($\mu = X_c/X_{L1}$) were computed by determining the eigenvalues of the Jacobian matrix evaluated at system equilibrium. The other operating parameters were kept constant ($T_m=0.91$ p.u., $V_0=1.0$ p.u. and $V_{ref}=1.0953$ p.u.).

Fig. 4 shows the oscillatory modes of the model. Supersynchronous and subsynchronous electrical modes have frequencies dependent on the series compensation factor. There are three torsional oscillation modes with frequencies of 24.7 Hz, 32.4 Hz and 51.1 Hz. The local swing mode has a frequency of 1.46 Hz. In the local swing mode, the turbine-generator shaft sections oscillate as a rigid body. In case the torsional modes are excited, on the other hand, some of the shaft masses oscillate against the others causing loss of fatigue life and eventually the shaft damage [22].

Hopf bifurcation points of the system are found by monitoring the real parts of the eigenvalues of the Jacobian matrix. As the series compensation factor is increased, the subsynchronous electrical mode frequency decreases and

interacts with all three torsional modes resulting in movement of the real part of the corresponding eigenvalue towards to the zero-axis, as shown in Fig. 5.

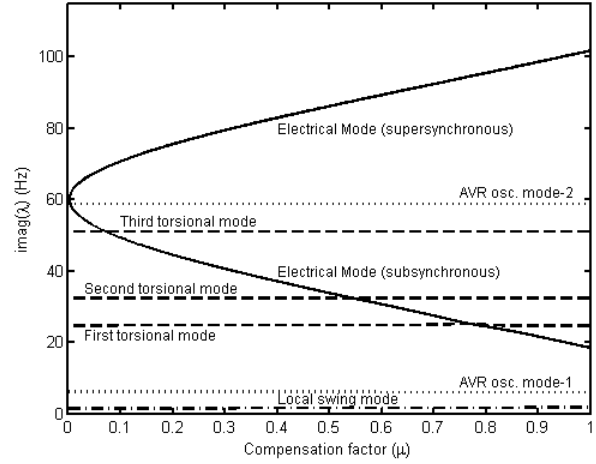


Fig. 4. Oscillatory modes of the model

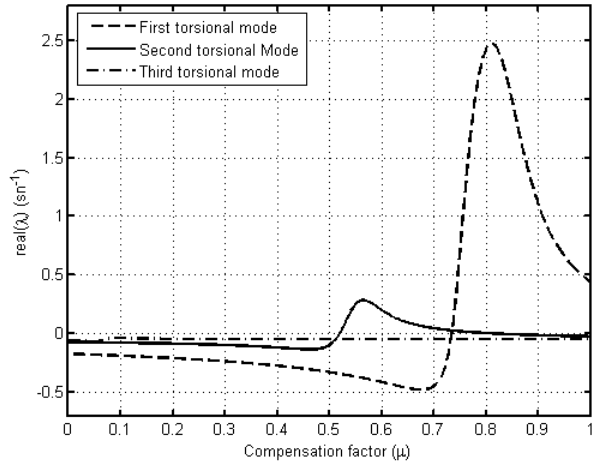


Fig. 5. Real parts of the torsional mode eigenvalues

The interaction with the third torsional mode occurs at $\mu = 0.0701$, without causing instability. The real part of the second torsional mode eigenvalue crosses the zero-axis at $\mu = 0.51968$, as a result of interaction with the subsynchronous electrical mode and the system stability is lost. Though the second torsional mode regains stability at $\mu = 0.81524$, the overall system stability is not regained because of the Hopf bifurcation occurring at $\mu = 0.73448$ in the first torsional mode which interacts strongly with the subsynchronous electrical mode.

4. Delayed Feedback Controller

The delayed feedback controller (DFC) consists of time delay, subtraction and gain operators. Fig. 6 shows the block diagram of the DFC. The synchronous generator rotor speed (ω_r) is used as input to the DFC block. The output signal is obtained by subtracting the τ delayed value of ω_r from its current value and then multiplying the result by a gain (K_{DFC}). V_s is then combined into the AVR as the stabilizing signal.

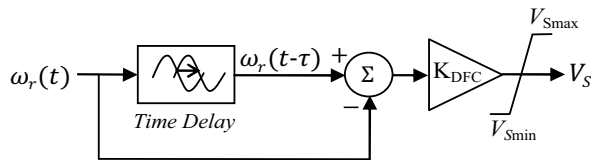


Fig. 6. Block diagram of the Delayed Feedback Controller

In order to study the dynamic response of the model in time domain, simulations in MATLAB-Simulink have been performed. At the system equilibrium with the operating values $T_m=0.91$, $V_0=1.0$ and $V_{ref}=1.0953$, a disturbance of 0.4 p.u. positive pulse torque was applied on the generator shaft at $t=1s$ for a duration of 0.5s ($\mu=0.55$).

The generator rotor speed response without DFC is obtained as shown in Fig. 7. Following the disturbance, the oscillations of the local mode of the generator are excited but they disappear. It is observed that the magnitude of torsional oscillations with frequency 32.4 Hz increases due to SSR. As a result, the system equilibrium is not reached because of the loss of stability through the Hopf bifurcation occurring at $\mu=0.52$. In such case, unless the synchronous generator is disconnected from the grid by means of protective devices (e.g. loss of synchronism, over-speed), catastrophic damage can occur.

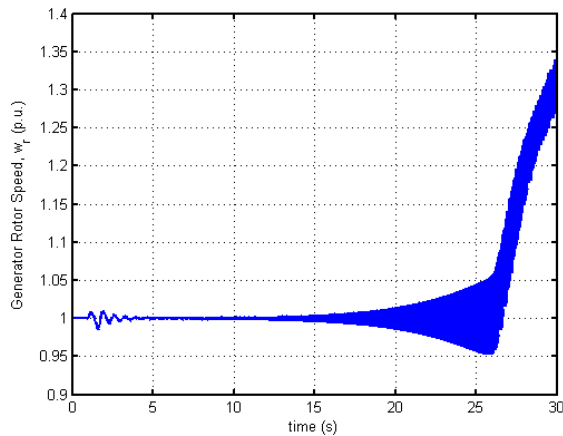


Fig. 7. Synchronous generator rotor speed response ($\mu=0.55$)

It is evident from Fig. 8 that the DFC successfully stabilizes the torsional oscillations due to SSR.

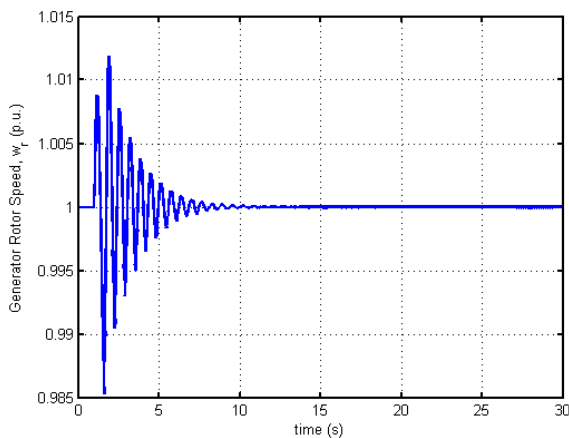


Fig. 8. Generator rotor speed with DFC ($\mu=0.55$, $\tau=0.018s$)

It is important to emphasize that analysis of nonlinear delay differential equations are extremely difficult. In order to investigate the DFC set parameters giving effective results, a performance index based on the evaluation of time domain responses is defined as follows:

$$P_{DFC}(\tau, K_{DFC}) = \max(\omega_r) - \min(\omega_r) \quad (21)$$

for $t_1 < t < t_2$. The time interval values t_1 and t_2 has been chosen as 8s and 10s, respectively.

As shown in Figs. 9-10 that there exists a correlation between the optimization performance index and the DFC parameters. The evaluated optimum set parameters are valid for the operating points at which the simulation is performed.

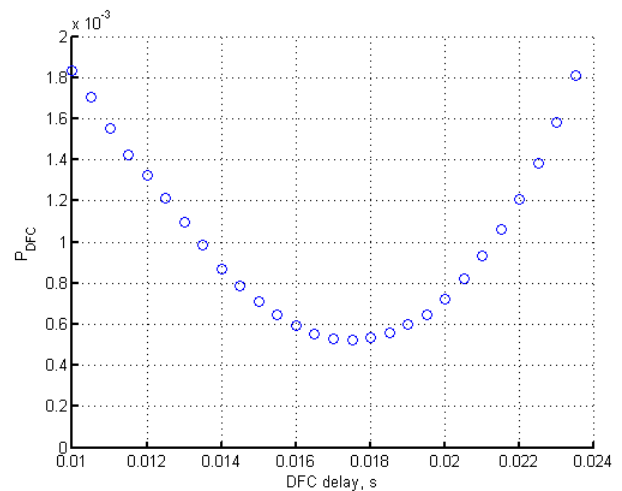


Fig. 9. DFC performance index ($\mu=0.55$, $K_{DFC}=70$)

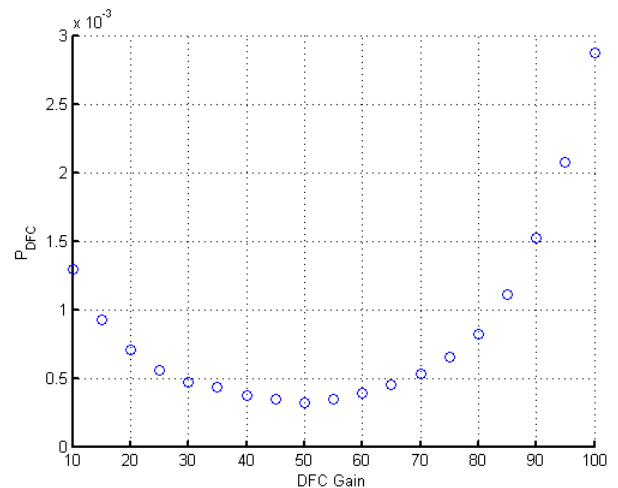


Fig. 10. DFC performance index ($\mu=0.55$, $\tau=0.018s$)

The DFC output limiters cut in during the initial period following the disturbance. Since the DFC uses the generator rotor speed as input, significant deviations mainly due to the local swing mode in this signal causes the DFC output limiters to cut in. Only after the oscillations at the local swing mode has decayed to a certain value, the DFC output limiters cut out. The generator terminal voltage reaches to a value of 1.19 p.u. momentarily.

5. Conclusions

The unstable torsional oscillations observed in the first system of the IEEE SBM can be stabilized by the delayed feedback controller which uses the synchronous generator rotor speed as the only input. The stabilizing output signal is combined into the AVR. The optimal values of the controller time delay and gain parameters have been determined by evaluating the dynamic response of the nonlinear model in time domain.

The merits of the proposed controller involve that it requires the measurement of only one observable state variable and the optimal setting of only two parameters, namely the time delay and the controller gain.

6. Appendix

Synchronous generator

$X_d=1.65$	$X'_d=1.59$	
$X_{akd}=1.51$	$X_{akq}=1.45$	
$X_{kkd}=1.642$	$X_{kkq}=1.5238$	
$X_{ffd}=1.6286$	$X_{afd}=1.51$	$X_{fkd}=1.51$
$r_a=0.0045$	$r_{fd}=0.00096$	
$r_{kd}=0.016$	$r_{kq}=0.0116$	

Network

$X_T=0.12$	$R_T=0.0012$
$X_{L1}=0.48$	$R_1=0.0444$
$X_{L2}=0.4434$	$R_2=0.0402$
$X_b=0.18$	$R_b=0.0084$

Mechanical System

$D_1=0.0498$	$M_1=0.498$	$K_{12}=42.6572$
$D_2=0.031$	$M_2=3.1004$	$K_{23}=83.3823$
$D_3=0.1758$	$M_3=1.7581$	$K_{34}=3.7363$
$D_4=0.0014$	$M_4=0.0138$	

Excitation System with AVR

$K_A=250, T_A=0.002$ s		
$K_E=1,$	$T_E=0.02$ s	
$K_F=0.03,$	$T_F=1$ s	$T_R=0.020$ s
$V_{Rmin}=-7.3$ p.u.,	$V_{Rmax}=7.3$ p.u.	

Delayed Feedback Controller

$V_{Smin}=-0.15$ p.u.	$V_{Smax}=0.15$ p.u.
-----------------------	----------------------

7. References

- [1] IEEE Committee Report, "Reader's Guide to Subsynchronous Resonance", *IEEE Trans. on Power Systems*, Vol. 7, No. 1, pp. 150-157, Feb.1992.
- [2] IEEE SSR Working Group, "First Benchmark Model for Computer Simulation of Subsynchronous Resonance", *IEEE Trans. Power Apparatus and Systems*, vol. 96, pp. 1565-1572, Sep.1977.
- [3] IEEE SSR Working Group, "Second Benchmark Model for Computer Simulation of Subsynchronous Resonance", *IEEE Trans. Power Apparatus and Systems*, vol. 104, pp. 1057-1066, May 1985.
- [4] P. M. Anderson, B. L. Agrawal and J. E. Van Ness, *Subsynchronous Resonance in Power Systems*, New York: IEEE Press, 1990, pp. 11-14.
- [5] I. M. Canay, "A novel approach to the torsional interaction and electrical damping of the synchronous machine, part I: Theory", *IEEE Trans. Power Apparatus and Systems*, vol. PAS-101, no. 10, pp. 3630-3638, Oct. 1982.
- [6] I. M. Canay, "A novel approach to the torsional interaction and electrical damping of the synchronous machine, part II: Application to an arbitrary network", *IEEE Trans. Power Apparatus and Systems*, vol. PAS-101, no. 10, pp. 3639-3647, Oct. 1982.
- [7] W. Zhu, R. R. Mohler, R. Spee, E. A. Mittelstadt, and D. Maratukulam, "Hopf Bifurcations in a SMIB Power System with SSR", *IEEE Transactions on Power Systems*, vol. 11, no. 3, pp. 1579-1584, Aug. 1996.
- [8] M. R. Iravani and A. Semlyen, "Hopf bifurcations in torsional dynamics", *IEEE Transactions on Power Systems*, vol. 7, no. 3, pp. 28-36, Feb. 1992.
- [9] A. M. Harb, "Application of Bifurcation Theory to Subsynchronous Resonance in Power Systems," Ph.D. dissertation, Dept. Electrical Eng., Virginia Polytechnic Institute and State Univ., Blacksburg, 1996.
- [10] R. G. Farmer, A. L. Schwab and E. Katz, "Navajo project report on subsynchronous resonance analysis and solution", *IEEE Trans. PAS*, vol. 96, no. 4, pp. 1226-1232, Jul 1977.
- [11] L. Wang, "Damping of torsional oscillations using excitation control of synchronous generator: the IEEE Second Benchmark Model Investigation", *IEEE Trans. on Energy Conversion*, vol. 6, No. 1, pp 47-54, Mar. 1991.
- [12] A. E. Hammad and M. El-Sadek, "Application of a thyristor controlled VAR compensator for damping subsynchronous oscillations in power systems", *IEEE Trans. PAS*, vol. 103, pp. 198-212, 1984.
- [13] K. R. Padiyar and N. Prabhu, "Design and Performance Evaluation of Subsynchronous Damping Controller with STATCOM", *IEEE Trans. on Power Delivery*, vol. 21, No. 1, pp 1398-1405, Jul. 2006.
- [14] N. G. Hingorani, "A New Scheme for Subsynchronous Resonance Damping of Torsional Oscillations and Transient Torque – Part I", *IEEE Trans. PAS*, vol. 100, no. 4, pp. 1812-1855, Apr. 1981.
- [15] A. M. Harb, M.S. Widyana, "Chaos and bifurcation control of SSR in the IEEE second benchmark model", *Chaos, Solitons and Fractals*, vol. 21, pp. 537-552, 2004.
- [16] K. Pyragas, "Continuous control of chaos by self-controlling feedback", *Physics Letters A*, 170, pp. 421-428, 1992.
- [17] K. Pyragas, V. Pyragas and H. Benner, "Delayed feedback control of dynamical systems at a subcritical Hopf bifurcation", *Physical Review E*, 70, pp. 056222:1-4, 2004.
- [18] A. Ahlborn and U. Parlitz, "Stabilizing unstable steady states using multiple delay feedback control", *Physical Review Letters*, vol. 93, pp. 264101-1-4, Dec. 2004.
- [19] T. Dahms, P. Hövel and E. Schöll, "Control of unstable steady states by extended time-delayed feedback", *Physical Review E*, vol. 76, pp. 056201-1-10, 2007.
- [20] A. M. Harb, M.S. Widyana, "Modern Nonlinear Theory as applied to SSR of the IEEE Second Benchmark Model", presented at the Bologna PowerTech Conference, Bologna-Italy, 2003.
- [21] *Recommended Practice for Excitation System Models for Power System Stability Studies*, IEEE Standard 421.5-1992, Aug. 1992.
- [22] P. Kundur, *Power System Stability and Control*, New York, Electric Power Research Institute, McGraw-Hill, 1994, pp 1061-1065.